Bioorganic & Medicinal Chemistry 20 (2012) 4348–4355

Contents lists available at SciVerse ScienceDirect

Bioorganic & Medicinal Chemistry

journal homepage: www.elsevier.com/locate/bmc

Myxobacteria versus sponge-derived alkaloids: The bengamide family identified as potent immune modulating agents by scrutiny of LC–MS/ELSD libraries

Tyler A. Johnson [a,b], Johann Sohn [a], Yvette M. Vaske [b], Kimberly N. White [b], Tanya L. Cohen [b], Helene C. Vervoort [b], Karen Tenney [b], Frederick A. Valeriote [c], Leonard F. Bjeldanes [a], Phillip Crews [b,*]

[a] Department of Nutritional Sciences & Toxicology, University of California, Berkeley, CA 94720, USA
[b] Department of Chemistry & Biochemistry, University of California, Santa Cruz, CA 95064, USA
[c] Josephine Ford Cancer Center, Henry Ford Health System, Detroit, MI 48202, USA

ARTICLE INFO

Article history:
Received 7 March 2012
Revised 8 May 2012
Accepted 17 May 2012
Available online 24 May 2012

Keywords:
Myxobacteria
Sponge
Bengamides
Anti-tumor
Inflammation
NF-κB
TNFα
IL-6
MCP-1

ABSTRACT

A nuclear factor-κB (NF-κB) luciferase assay has been employed to identify the bengamides, previously known for their anti-tumor activity, as a new class of immune modulators. A unique element of this study was that the bengamide analogs were isolated from two disparate sources, *Myxococcus virescens* (bacterium) and *Jaspis coriacea* (sponge). Comparative LC–MS/ELSD and NMR analysis facilitated the isolation of *M. viriscens* derived samples of bengamide E (**8**) and two congeners, bengamide E′ (**13**) and F′ (**14**) each isolated as an insperable mixture of diastereomers. Additional compounds drawn from the UC, Santa Cruz repository allowed expansion of the structure activity relationship (SAR) studies. The activity patterns observed for bengamide A (**6**), B (**7**), E (**8**), F (**9**), LAF 389 (**12**) and **13**–**14** gave rise to the following observations and conclusions. Compounds **6** and **7** display potent inhibition of NF-κB (at 80 and 90 nM, respectively) without cytotoxicity to RAW264.7 macrophage immune cells. Western blot and qPCR analysis indicated that **6** and **7** reduce the phosphorylation of IκBα and the LPS-induced expression of the pro-inflammatory cytokines/chemokines TNFα, IL-6 and MCP-1 but do not effect NO production or the expression of iNOS. These results suggest that the bengamides may serve as therapeutic leads for the treatment of diseases involving inflammation, that their anti-tumor activity can in part be attributed to their ability to serve as immune modulating agents, and that their therapeutic potential against cancer merits further consideration.

Published by Elsevier Ltd.

1. Introduction

We believe that the side-by-side exploration of sponges and myxobacteria for bioactive secondary metabolites can be rewarding. Marine sponges are now recognized as a superb source of physiologically active compounds possessing immense structural diversity.[1] Likewise, some myxobacteria also elaborate heteroatom-rich bioactive secondary metabolites,[2] including some that have been the seeds for developing clinically useful therapeutics.[3] The success, from 1970–2010, by Höfle and Reichenbach at HZI (formerly the GBF) in isolating chemically prolific strains from this group has been captivating.[2] Of special interest to us are examples, though few in number, of myxobacterial secondary metabolites possessing nearly identical molecular structures and biological functions compared to those of sponge-derived products. Shown in Figure 1 are two such parallelisms which intimate the possibility of congruent biosynthetic machinery operating in these very different biota. The F-actin stabilizers,[4] jasplakinolide[5] (a.k.a. jaspamide[6]) (**1**), from a *Jaspis splendens* sponge,[7] versus chondramide D[4,8–10] (**2**), from the myxobacterium, *Chondromyces crocatus*[11] illustrate parallel biogenesis that involves halogenation, fusion of a tetraketide to a tripeptide, and macrocyclization. As another similar example, there is just one biogenesis difference, consisting of the presence or absence of the heteroatom ring, between the Vacuolar ATPase inhibitors[12] salicylihalamide (**3**) from a *Haliclona* sponge genus[13] compared to apicularen A (**4**), from the myxobacterial genus *Chondromyces*.[14]

Even though few salt-obligate marine myxobacteria have been isolated,[15–18] the origin of shared biosynthetic machinery for the pairs of natural products summarized above remains a fascinating mystery. This stimulated our quest to probe the chemical biology of marine sponges and terrestrial myxobacteria that appear to share identical biosynthetic machinery. A serendipitous opportunity, which involved interfacing this interest with the goals of an International Cooperative Biodiversity Group (ICBG) project to investigate natural products with immune modulating activity,[19] resulted in the accumulation of promising data. The evaluation of 128 myxobacterial extracts in a nuclear factor kappa B (NF-κB) luciferase assay[20] provided the motivation to further explore the

* Corresponding author. Tel.: +1 831 459 2603.
E-mail address: pcrews@ucsc.edu (P. Crews).

0968-0896/$ - see front matter Published by Elsevier Ltd.
http://dx.doi.org/10.1016/j.bmc.2012.05.043

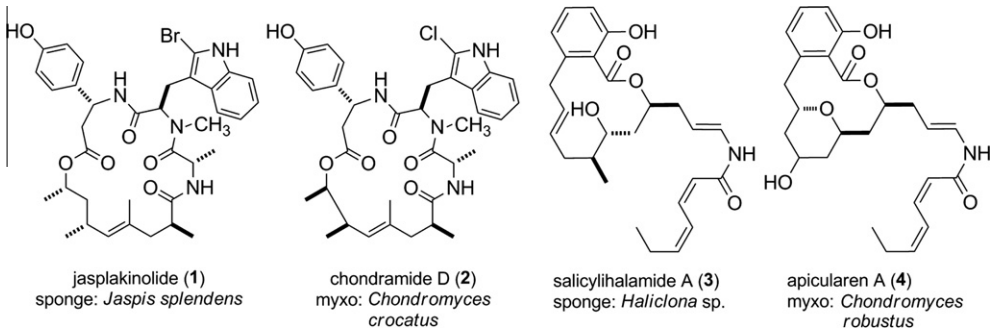

Figure 1. Structural similarities between sponge-derived and myxobacteria-derived compounds.

bioactive constituents of selected strains. Dysregulation of the NF-κB protein complex is pathogenic in a wide variety of diseases including AIDS,[21] Alzheimers disease,[22] artherosclerosis,[23] arthritis[24] and cancer.[25,26] Since NF-κB has been implicated in many diseases it is now considered to be an important therapeutic target for drug discovery.[27]

The five proteins in the mammalian NF-κB family are divided into two classes and in the last decade intensive efforts have gone into the discovery of small molecule inhibitors. These transcription regulating proteins, two denoted as NF-κB's and three referred to as Rel's, are held in the cytoplasm in an inactive state by an inhibitory subunit called IκB (inhibitory protein of the nuclear factor κB).[28] Phosphorylation of IκB and its subsequent degradation allows for translocation of NF-κB to the nucleus. Further, NF-κB activation in cells is stimulated by pro-inflammatory agents such as bacterial endotoxins (e.g., lipopolysacharide, LPS), cytokines, chemokines, carcinogens or oxidative stress. The substantial efforts to explore NF-κB inhibitors includes 125 compounds reported in 1999[29] to the nearly 1000 to date, collectively summarized by the Gilmore lab.[30] A vast majority are natural products of plant biosynthetic origins,[31] but very few exhibit low nM inhibition of NF-κB signaling.[30] One noteworthy exception is celastrol (**5**),[32] which is being pursued as an important anti-arthritic and anticancer therapeutic lead based on its impressive activity in vivo.[33,34]

A dichloromethane extract from a myxobacterium, *Myxococcus virescens* coded DSM 15898 FD, screened in the NF-κB luciferase assay during our ICBG collaboration, exhibited anti-inflammatory effects comparable to celastrol (**5**) with no cytotoxicity to macrophage (RAW 264.7) immune cells (see Fig. S1, Supplementary data). Secondary metabolites of this *M. virescens* strain have been reported only in the patent literature and include bengamide E (**8**) and other analogs.[35] These preliminary results provided the justification to launch a campaign, conducted in three phases, to examine the basis for the NF-κB luciferase assay result. These actions involved: (1) identifying the metabolites in the extract responsible for the anti-inflammatory activity, (2) side-by-side comparison of the myxobacterial bengamides to analogs purified from the Indo Pacific sponge *Jaspis coriacea*,[36–39] and (3) mechanistic investigation of the signal transduction pathways targeted by the active compounds effecting NF-κB signaling. Herein, we report on the absolute configurations of the myxobacterial derived bengamides. We also show that the bengamides exhibit nM inhibition of NF-κB in RAW 264.7 cells and that this effect is associated with the inhibition of phosphorylation of IκBα, and the reduced expression of the pro-inflammatory cytokines/chemokines tumor necrosis factor α, (TNFα), interleukin-6 (IL-6) and monocyte chemotactic protein-1, (MCP-1).

2. Results and discussion

To rapidly pinpoint the metabolites responsible for the observed activity of the *M. virescens* extract coded DSM 1598FD in the NF-κB luciferase assay[20] we began by using the previously reported LC–MS/ELSD based peak-library approach.[19] Shown in Figure 2 are the overlaying of peaks visualized by LC–MS/ELSD with data obtained from the NF-κB luciferase assay. Several fractions displayed potency greater than the standard celastrol (**5**, 250 nM) (Fig. 2) and include: H17 (341 *m*/*z*), H18 (245 *m*/*z*) H19 (355 *m*/*z*), H20 (369 *m*/*z*), and H36 (416 *m*/*z*). The components exhibited *m*/*z* ions $[M-H_2O+H]^+$ that corresponded to bengamide E (**8**, 341 *m*/*z*),[38] F (**9**, 355 *m*/*z*),[38] a simple diketopiperazine (cyclo-Pro-Phe, 245 *m*/*z*, $[M+H]^+$), and a unique *m*/*z* = 369 and 416. Scale up, reverse phase HPLC of the parent dichloromethane (375.4 mg) and methanol (191.2 mg) extracts was needed to provide more of the minor metabolites, especially the 341 *m*/*z* and of 369 *m*/*z* components for further structural and bioassay analysis. Eventually semipure fractions of these metabolites were obtained (see Scheme S1, Supplementary data). Fraction H36 exhibited chemical shifts and a *m*/*z* ion = 416 unrelated to the bengamide class and is currently under investigation.

The process of correlating the myxobacterial metabolites with those of sponge-derived counterparts warrants elaboration. The 341 *m*/*z* metabolite displayed an LC–MS retention time parallel to the sponge-derived compound bengamide E (**8**), as shown Figure S2. Final dereplication of this compound was based on the molecular formula of $C_{17}H_{30}N_2O_6$ established from HRESITOFMS *m*/*z* 381.2010 $[M+Na]^+$, and ^1H NMR spectrum of this sample (Fig. S3) which showed minor impurities alongside diagnostic δ_H values that exactly matched those of bengamide E (**8**).[38] Our analysis clearly indicated that the terrestrial myxobacterium and marine sponge produced identical compounds.

The fraction coded as H19 (355 *m*/*z*) was a major metabolite, eventually concluded to be bengamide E′ (**13**), which shared an LC–MS retention time equivalent to that of sponge-derived bengamide F (**9**) (see in Fig. S4). However, it quickly became evident that this compound was a homologue of **8**. The ESI–TOF-HRMS formula of $C_{18}H_{33}N_2O_6$, for fraction H19, while identical to that of **9** exhibited NMR resonances that were markedly different (see Fig. S5). After repeated injections using either an analytical 5 μ reverse phase or chiral HPLC column we concluded that this fraction contained an inseparable mixture of diastereomers at position C-2 (ratio of 60:40, see Fig. S19). Further inspection of the 1D and 2D NMR data (shown in Table S1 and Figs. S6–S10) indicated these diastereomers, relative to bengamide E (**8**), were chain extended by an extra carbon on the left end and are named here as bengamide E′ (**13**). Most of the ^1H NMR resonances at this terminal end were doubled (Fig. S19) including those of the C_2H_5 group labeled R4 (Table 1), the CH_3-15, and the vinyl group, H-4, and H-5. In comparison to bengamide E (**8**), of absolute configuration 5*R*, 6*S*, 7*R*, 8*R*, and 10*S*, the new analogue is assigned to have the same features. However, the terminal end methylation appears to have been biosynthetically introduced in a scalemic fashion, which is consistent with multiple resonances for the residues in the vicinity

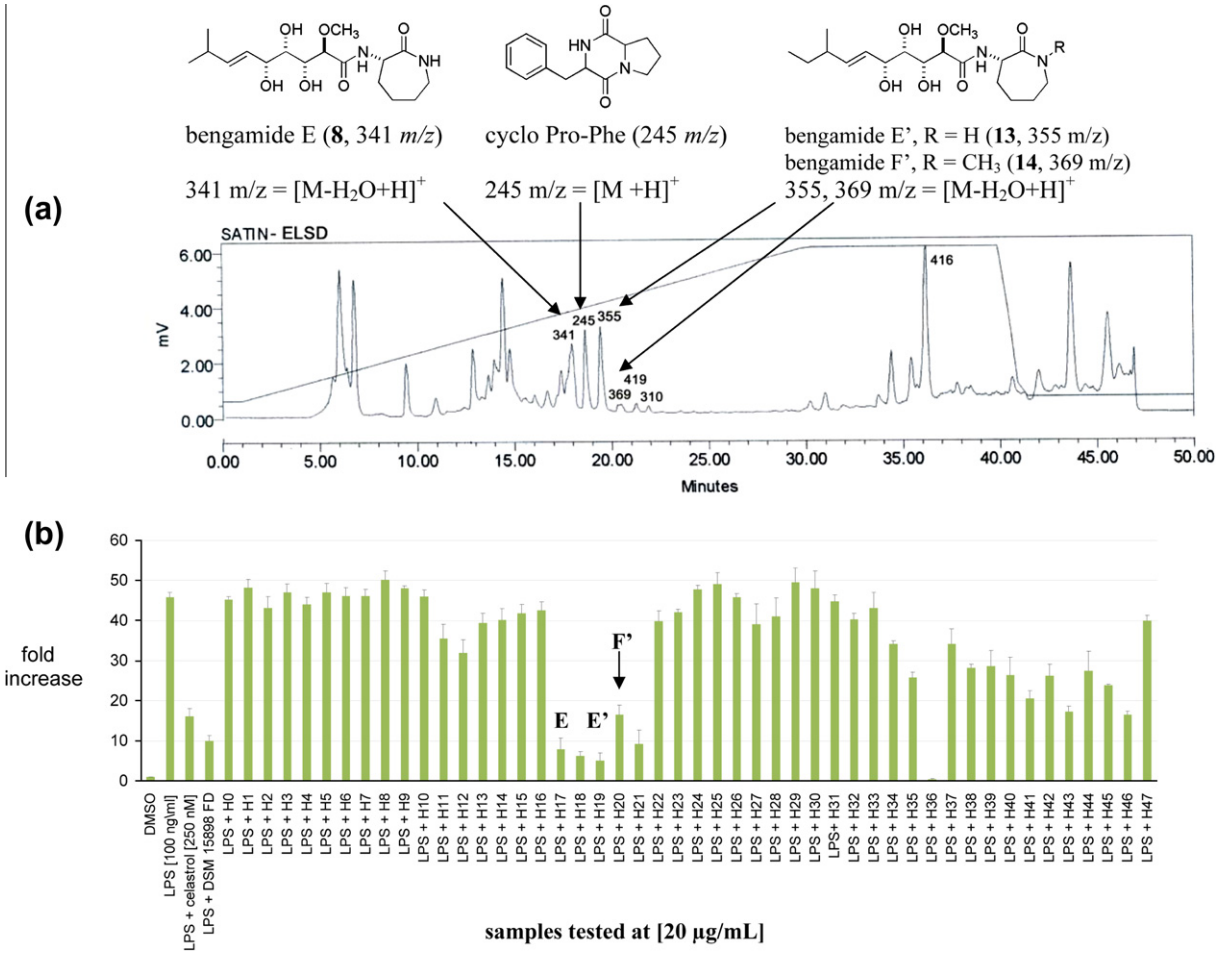

Figure 2. Observed LC–MS/ELSD peak-library trace with selected annotations including: (a) *m/z* ions associated with key metabolites, and (b) NF-κB inhibition responses modulated by celastrol (**5**) measured in the luciferase assay of *M. virescens* (extract coded DSM 15898 FD) LC peak-library fractions.

of this additional methyl. Analysis of literature ^{13}C NMR shifts provides a diagnostic pattern, shown in Figure 3, to further address the configurations at these centers noted above. The comparison of Panel A plots differences in ^{13}C shifts of natural bengamide E (**8**) from *J. coriacea*[36] versus data published for **8** from three different enantiospecific total syntheses;[40–42] and documents that the variation in shifts at each site is <1 ppm. By contrast, the information of Panel B shows that modification of the absolute configurations at C-6 and C-7 in the synthetic **8** diastereomer of 5*R*, 6*R*, 7*S*, 8*R* configuration, also obtained by an enantiospecific total synthesis,[43] imparts a >1 ppm change in the ^{13}C NMR chemical shifts at the 3/4 sites. Finally, Panel C illustrates the close parallelisms in shifts of the following set: (a) natural bengamide E (**8**), synthetic bengamide E (**8**), (c) natural bengamide E′ (**13**) as a diastereomeric mixture, and (d) synthetic E′ (**13**) reported from a scalemic total synthesis.[41]

The active metabolite in fraction H20 (369 *m/z*) displayed properties similar to those of **13**. Its formula, $C_{19}H_{34}N_2O_6$, established by HRMS alongside the ^1H NMR spectrum indicated this was the *N*-methyl homologue of **13**. It was named bengamide F′ (**14**), also isolated as a mixture of diastereomers epimeric at position C-2. The configurations assigned of **14** were based on a biosynthetic analogy to the co-occuring metabolite **8** with absolute configurations 5*R*, 6*S*, 7*R*, 8*R*, and 10*S*.

The preliminary assay data of Figure 2 showed a large inhibition in the initial NF-κB screen of the LC–MS/ELSD fractions H17, H19, and H20 containing the compounds discussed above. This provided the motivation to more fully assess the quality of these biological responses. Also important was that the cytotoxicity data obtained against macrophage immune (RAW 264.7) cells for these same fractions (see Supplementary data Fig. S1) indicated selectivity. Next, these two screens were repeated on purified compounds to determine IC_{50} values. This evaluation was conducted on the following compounds: (a) assay standard, celastrol (**5**); (b) the myxo-derived bengamides E (**8**), E′ (**13**), F′ (**14**); (c) the sponge-derived compounds obtained from our repository of bengamide A (**6**), B (**7**), E (**8**), F (**9**); and (d) a synthetic bengamide analog, LAF-389 (**12**),[44] previously evaluated by Novartis in a Phase I clinical trial for the treatment of advanced cancer.[45] Data was also collected to assess the IC_{50} inhibition of cultured human colon tumor (HCT-116) cell lines by this compound collection as shown in Table 1. All compounds exhibited significant NF-κB inhibition as shown by the IC_{50} values (in parentheses) versus their toxicity assessment against RAW 264.7 cells ($\geqslant$50 μM). The two most active analogs consisted of **6** (0.08 μM) and **7** (0.09 μM), which displayed low nanomolar activity compared to celastrol (**5**, 0.2 μM). Compounds **8**–**9** and **12**–**14** (7.5, 0.7, 0.5, 2.0, 2.0 μM) were less NF-κB inhibitory suggesting a significant role of the myristate moiety in enhancing the potency of the NF-κB inhibition. A similar trend was also observed for the presence and absence of the myristate and its impact on the IC_{50} potencies of these various bengamide compounds against the HCT-116 cell lines.

An extensive investigation using a proteomics approach has identified that **12** targets both isoforms of human methionine aminopeptidase (MetAps 1 and 2) proteins.[46] Further investigations

Table 1
The comparative NF-κB inhibition, RAW 264.7 cell toxicity, and tumor cell cytotoxicity for celestrol (**5**) and bengamide analogs (**6**–**14**)

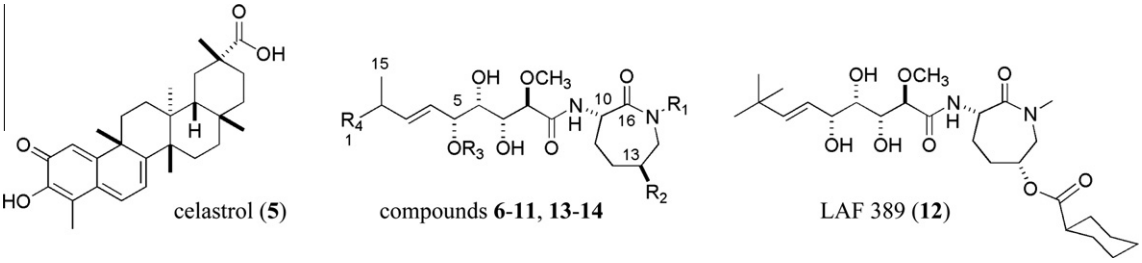

Compound	NIH NSC[a]	R_1	R_2	R_3	R_4	NF-κB[b] IC_{50} (μM)[e]	RAW 264.7[c] IC_{50} (μM)[e]	HCT-116[d] IC_{50} (μM)[e]
Celastrol (**5**)	70931					0.200[d]	>50.0[d]	NA[f]
Bengamide A (**6**)	613012	H	$OC(CH_2)_{12}CH_3$	H	Me	0.075[d]	>50.0[d]	0.018[g]
Bengamide B (**7**)	646846	Me	$OC(CH_2)_{12}CH_3$	H	Me	0.085[d]	>50.0[d]	0.002[g]
Bengamide E (**8**)	none	H	H	H	Me	7.5[d]	>50.0[d]	0.06[h]
Bengamide F (**9**)	666195	Me	H	H	Me	0.7[d]	>50.0[d]	NA[f]
Bengamide P (**10**)	646847	H	H	$OC(CH_2)_{12}CH_3$	Me	NA[f]	NA[f]	0.73[g]
Bengamide Z (**11**)	716230	Me	OH	H	Me	NA[f]	NA[f]	10.3[i]
LAF 389 (**12**)	none					0.5[d]	>50.0[d]	0.04[h]
Bengamide E′ (**13**)	750259	H	H	H	CH_2CH_3	2.0[d]	>50.0[d]	1.1[d]
Bengamide F′ (**14**)	none	Me	H	H	CH_2CH_3	2.0[d]	>50.0[d]	1.5[d]

[a] National institute of health (NIH) NSC number.
[b] NF-κB inhibition measured using an LPS-induced NF-κB luciferase assay with RAW 264.7 cells—18 h.
[c] Cytotoxicity measured against murine macrophage (RAW 264.7) cell lines—18 h.
[d] This work.
[e] The values (IC_{50}) represent the mean ± SE for $n = 3$.
[f] Not available (NA) for evaluation.
[g] Thale et al., **2001**, *J. Org. Chem. 66*, 1733–1741.
[h] Novartis Institute for Biomedical Research (NIBR) personal communication.
[i] Groweiss et al., **1999**, *J. Nat. Prod., 62*, 1691–1691.

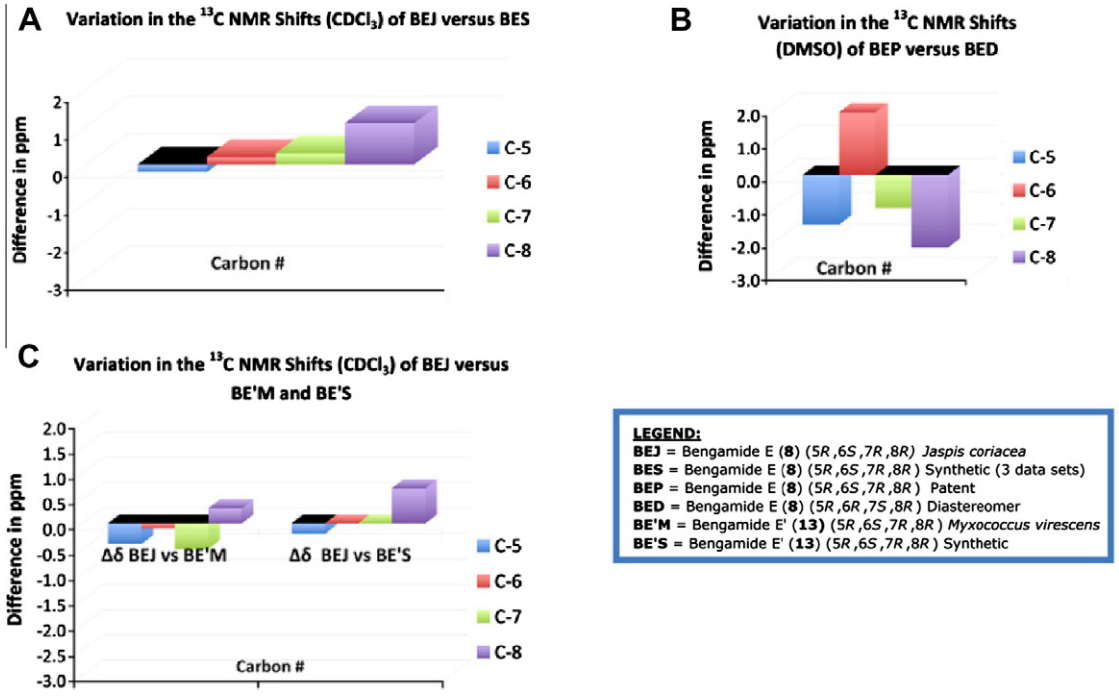

Figure 3. Comparative ^{13}C NMR chemical shifts of naturally occurring and synthetic bengamide E (**8**), diastereotopic mixture of E′ (**13**) showing parallelisms to justify assignment of the absolute configurations assigned at C5, C6, C7, C8 for **13**.

have shown that inhibition of MetAPs by **6** led to the regulation of *c*-Src non-receptor tyrosine kinase activity.[47] Additional perspectives based on the two different sets of bioactivity properties of **6**–**7** and analogs merits comment. First, the profiles of **6**–**7** in the

NCI 60 cell-line are unique compared to most other compounds in the NCI database, suggesting that the bengamides perturb undescribed molecular targets. Ascribing their anti-tumor activity to direct effects on MetAPs does not seem to provide a complete picture.[47] More recently, the bengamide class has shown promise for the treatment of tuberculosis as lead compounds based on this scaffold have the potential to selectively inhibit *M. tuberculosis* MetAPs vs human MetAPs.[48] It is unclear the extant that such targets[49] may account for their anti-inflammatory properties. On the one hand we hypothesized that the anti-inflammatory properties of the bengamides are probably, or at least partially, also responsible for their anti-tumor activities due to the close link between tumorigenesis and inflammation.[50,51] Ongoing studies into the molecular targets of the bengamides responsible for their biological activity affecting cancer and other diseases indicated that further exploration of the role(s) they may play in the immune pathway could be useful. Thus, the next step in this project involved a more thorough study on the effects of the bengamides on the signaling pathways that target NF-κB.

The NF-κB inhibitory activity of the bengamides A (**6**), B (**7**), E (**8**) and F (**9**) were evaluated by Western Blot analysis shown in Figure 4, analyzing the degree of inhibition of phosphorylation of IκBα, a common indicator of NF-κB inhibition.[28,52] With increasing concentrations of **6**–**9**, there is a clear decrease in the levels of observed IκBα phosphorylation. Also shown by these data is that bengamide A (**6**) and B (**7**) are more effective than E (**8**) and F (**9**). These Western immunoblot results, in combination with the NF-κB luciferase assay, establish that the bengamide pharmacophore inhibits NF-κB activation. Next the inhibitory effects of **6** and **7** on LPS stimulated nitric oxide (NO) production and the pro-inflammatory cytokines/chemokines: inducible nitric oxide synthase (iNOS), TNFα, IL-6 and MCP-1 were evaluated and these results are shown in Figure 5. Neither **6** nor **7** showed NO inhibition activity or an effect on iNOS expression (data not shown) at concentrations up to of 10 μM. Alternatively both compounds displayed significant inhibition in a dose dependent manner against TNFα (**6**, IC_{50} ~0.5 μM; **7**, IC_{50} ~0.5 μM), IL-6 (**6**, IC_{50} ~1.0 μM; **7**, IC_{50} ~0.5) and MCP-1 (**6**, IC_{50} ~0.5 μM; **7**, IC_{50} ~0.5 μM). The expression of TNFα,[53,54] IL-6,[55,56] and MCP-1[57,58] are all closely linked to diseases involving inflammation and cancer. The above results should now be considered alongside additional findings that both the full bengamide structure[46] as well as modified synthetic bengamide analogs modulate methionine aminopeptidases.[59] Overall we believe that the bengamides affect key targets in the immune pathway and perhaps others that are also responsible for their anti-tumor activity.

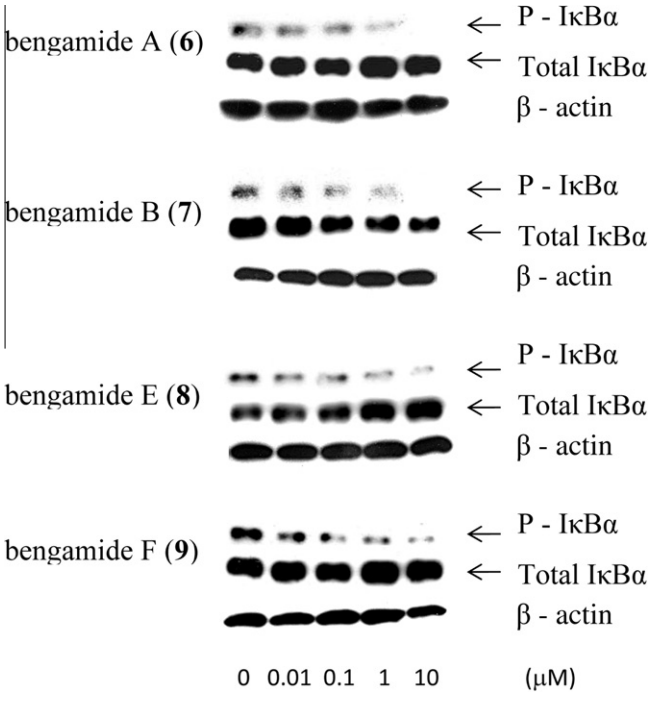

Figure 4. Western blot analysis of bengamide A (**6**), B (**7**), E (**8**) and F (**9**) at varying concentrations and their suppression of phosphorylation of IκBα with β actin as a control.

3. Conclusions

Several noteworthy conclusions can be drawn from our investigation of biologically active myxobacteria-derived extracts. The first is that bengamide E (**8**) and analogs E′ (**13**) and F′ (**14**) are in fact produced by *M. virescens*. With the exception of makaluvamine A, (isolated from the sponge *Zyzzya fuliginosa*[60] and myxomycetes 'slime mold' *Didymium bahiense*[61]) to the best of our knowledge this is only the second example in the peer-reviewed literature of a sponge-derived natural product reported from a cultured microbial source. This is intriguing in that, of the thousands of compounds isolated from sponges, a vast majority are presumed to owe their biosynthetic origins to the sponges microbial symbionts[62] but few examples exist. Furthermore, this finding underscores the potential future discoveries that can come from the investigation of myxobacterial cultures.[2] A second important discovery is that the bengamides behave as immune modulating agents with respect to their inhibition of NF-κB without accompanying cytotoxicity to RAW 264.7 immune cells. Structure activity relationship studies revealed that bengamide A (**6**) and B (**7**) are the most potent at 80–90 nM, respectively. This class may therefore be able to serve as therapeutic leads for immune disorders involving inflammation as they possess activity on par with some of the most potent NF-κB inhibitors. Subsequent qPCR analysis indicated that the bengamides modulate the expression of the pro-inflammatory cytokines, TNFα,[53,54] IL-6,[55,56] and MCP-1[57,58] and that their effects on these targets might also contribute to their significant anti-tumor activity. Additional studies into the effects of bengamides involving the NF-κB pathway may uncover new targets for this class to serve as molecular probes whereas they currently provide a unique scaffold to develop a novel class of MetAP inhibitors for anti-bacterial, anti-tubercular and anti-cancer therapeutics.[46,48,59] In summary, we have identified the bengamides as potent immune modulating agents from the investigation of an extract of *M. virescens*. Our results suggest that further exploration into myxobacterial derived secondary metabolite chemistry is warranted and has the potential to uncover new interesting molecular structures that can be provided in a sustainable fashion through fermentation and go on to serve as important therapeutic leads for the treatment of a wide variety of human diseases.

4. Experimental section

4.1. General experimental procedures

Analytical LC–MS analysis was performed on samples at a concentration of approximately 5 mg/mL, using a reversed-phase 150 × 4.60 mm, 5 μm C_{18} Phenomenex Luna column in conjunction with a 4.0 × 3.0 mm C18 (Octadecyl) guard column and cartridge (Holder part number: KJ0-4282, Cartridge part number: AJ0-4287, (Phenomenex, Inc., Torrance, CA). Samples were injected onto the column using a volume of 15 μL, with a flow rate of 1 mL/min that was monitored using a Waters model 996 photodiode array (PDA) UV detector. The elution was subsequently split (1:1)

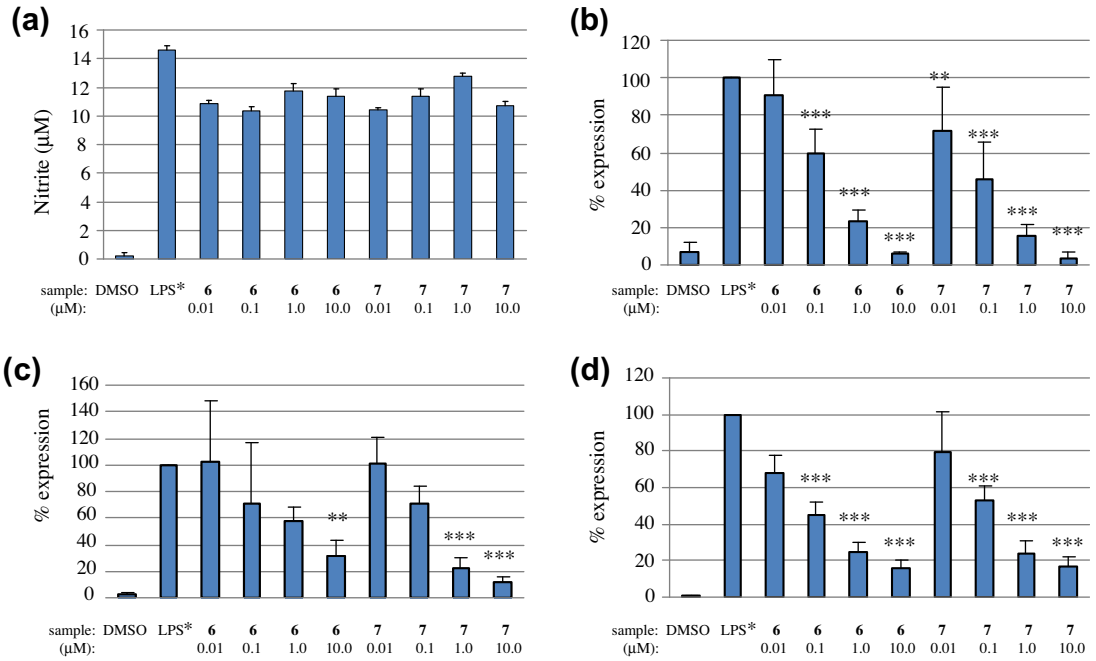

Figure 5. Effects of bengamide A (**6**) and B (**7**) on the inhibition of lipopolysacharide (LPS) induced expression of: (a) nitrous oxide (NO), (b) tumor necrosis factor (TNFα), (c) interleukin-6 (IL-6) and (d) monocyte chemotactic protein-1 (MCP-1) as measured by qPCR. *LPS (100 ng/mL) is used as a positive control and added to (0.01–10 μM) samples of **6** and **7**. Data are presented as mean ± SEM of three independent experiments.**$p < 0.05$, ***$p < 0.001$.

between a S.E.D.E.R.E. model 55 evaporative light scattering detector (ELSD), and an Applied Biosystems Mariner electrospray ionization time of flight (ESI–TOF) mass spectrometer. All NMR experiments were run on a Varian INOVA 600 spectrometer (600 and 150 MHz for ^{1}H and ^{13}C, respectively).

4.2. Biological material, collection and identification

Specimens of the myxobacteria strain DSM 15898 were obtained from the Deutsche Sammlung von Mikroorganismen und Zellkulturen (German Collection of Microorganims and Cell Cultures) taxonomically identified as *M. virescens* as reported previously.[35]

4.3. Pure compounds

Celastrol (**5**) was obtained from Cayman Chemical Company, Ann Arbor, MI, USA. Bengamide A, B, E and F (**6**–**9**), were obtained from the UCSC marine natural products repository from specimens of *J. coriacea* using methods reported previously.[36] Additional amounts of bengamide A (**6**) and (**7**) were supplied by C-GRO Biosciences, Santa Cruz, CA, USA. LAF-389 (**12**) was provided by Novartis Institutes for Biomedical Research (NIBR).

4.4. Extraction and prefractionation

We obtained DSM15898 from the Deutsche Sammlung von Mikroorganismen und Zellkulturen. It arrived as freeze-dried cells which were taken up in a minimum amount of sterile water and spread onto VY2 agar plates (pH 7.2). Bright yellow fruiting bodies formed after approximately one week at 30 °C. Agar plugs were transferred to six 1 L fermentations of MD1 media augmented with 20 mL of XAD-16 resin and 2.0 g baker's yeast (pH 6.8). Fermentation proceeded at 30 °C with orbital shaking at 120 rpm. After two weeks, the resin and fruiting bodies were filtered away from the broth and first extracted with 500 mL of methanol and then 500 mL of acetone. The extracts were combined and concentrated in vacuo. The residue was subjected to a modified Kupchan extraction scheme, as often employed in our previous works.[63] The culture broth was extracted using the following partition scheme involving hexanes (sample coded FH 82.4 mg), methanol, (sample coded FM, 239.9 mg) and dichloromethane (sample coded FD, 375.4 mg). A separate 1 L liquid culture was prepared according to the above protocol and following two weeks of incubation the resin and fruiting bodies were filtered away. The broth was extracted with hexanes, methanol and dichloromethane yielding the following extract: FH, 21.3 mg, FM, 191.2 mg and FD, 279.9 mg.

4.5. LC–MS/ELSD library fraction collection and scale up isolation

A [15.0 mg/150 μL] sample of the dichloromethane extract (sample coded DSM 15898 FD) was used to prepare a standard LC–MS/ELSD library for bioassay evaluation using methods reported previously.[19] Gradient conditions involved using H2O: CH_3CN (with 0.1% formic acid) consisting of 10:90→100% over 30 min. A duplicate library was then made using a 12-channel pipette, creating an exact copy and counter balance for analytical reference and centrifugal drying. Plates were dried and concentrated using a Savant AES2010 SpeedVac.

Bengamide E (**8**) was obtained by a 1 L grow up procedure shown in Scheme S1. From the FM fraction, 34 mg was subjected to HPLC with the elution subsequently split (1:1) between a S.E.D.E.R.E. model 55 evaporative light scattering detector (ELSD), and a Gilson 215 liquid handler controlled with Gilson Unipoint LC software. The sample was purified using a Phenomenex Luna (5μ C18 150 × 4.60 mm employing a gradient 5:95%→40% CH_3CN:H_2O (40 min) with buffered conditions using NH_4OAc, pH 8.8, Et_3N to generate H24 bengamide E (**8**, 2.2 mg) (R_t = 24.5 min) with spectroscopic data identical to that reported in the literature and ESI–TOF-HRMS $[M+Na]^+ = C_{17}H_{30}N_2O_6Na$, Calcd, 381.19961. Found, 381.20105 (error = 3.78232 ppm).

Preparative (P) scale up HPLC isolation of bengamide E′ (**13**) from the crude extract DSM 15898 FD (375.4 mg) involved 7 injections of a [50 mg/500 μL] solution using a Phenomenex Synergi (250 × 21.2 mm, 10 micron) column at a flow rate of 10 mL/min. using solvent conditions of 10:90→100% CH_3CN:H_20 (30 min) to generate five P fractions. Fraction P2 (167.2 mg) was subjected to repeated reverse phase HPLC using a Luna 5 μm, C18(2) 100 Å 10 × 250 mm column (Phenomenex, Inc., Torrance, CA) in conjunction with a guard column using a larger 10.0 × 10.0 mm C18 (ODS) cartridge (Holder part number: AJ0-7220, Cartridge part number: AJ0-7221) using the solvent conditions above. The fractions were monitored with a S.E.D.E.R.E. model 55 evaporative light scattering detector (ELSD) to generate a pure product P2H4 containing bengamide E′ (**13**, 31.8 mg**)**. Fraction P2H5 (4.4 mg) was further purified using a reversed-phase 150 × 4.60 mm 5 μm C_{18} Phenomenex Luna column with a gradient of 5:95% → 40% CH_3CN:H_2O (40 min) with buffered conditions using NH_4OAc, pH 8.8, Et_3N to generate P2H5H2 bengamide F′ (**14**, 1.4 mg).

4.6. NF-κB luciferase and human colon tumor (HCT) 116 assay

Extracts and pure compounds were tested in an NF-κB luciferase reporter assay in mouse macrophage (RAW264.7) immune cells to determine NF-κB activity. The RAW 264.7 cells were plated as 5×10^4 cells per well plate. Stably transfected RAW264.7 cells with the NF-κB reporter gene were plated in 96-well plates. Following a 24 h recovery period, the cells were treated with the extract(s) or compound(s) for an additional 18 h in the presence of LPS (100 ng/mL). To check NF-κB -luciferase activity, the Luciferase Reporter Assay System purchased from Promega (Madison, WI) were used. Cell lysates (15 μL) from treated RAW264.7 cells were placed in opaque 96-well plates. Luciferase Assay Reagent (50 μL) was injected and read by a fluorometer (LMAX 2, Molecular devices). The values (IC_{50}) represent the mean ± SE for $n = 3$. The IC_{50} values reported against HCT cell lines were obtained using methods described previously.[64]

4.7. Determination of phosphorylation of IκBα by western blot analysis

RAW264.7 cells were cultured in 6-well plates to near confluency, treated with increasing concentrations of compounds in the presence of LPS and incubated at 37 °C for 4 hr. Cells were immediately harvested in 200 μL of loading buffer (10% glycerol, 5% 2-mercaptoethanol, 10% SDS, 0.125 M Tris–HCl pH 6.7, 0.15% bromophenol blue), sonicated for 15 s, heated to 99.9 °C for 5 min and fractionated by electrophoresis on 4–15% polyacrylamide, 0.1% SDS resolving gels (BioRad). Proteins were electrically transferred to Immobilon-II membranes (Millipore, Billerica, MA), and blocked at room temperature for 1 h with 5% non-fat dry milk in wash buffer (10 mM Tris–HCl, pH 8.0, 150 mM NaCl, 0.05% Tween 20). Blots were subsequently incubated with antibodies against mouse phosphor-IκBα and IκBα (Cell Signaling, 1:1000). Immunoreactive proteins were detected after 1 h of incubation at room temperature with appropriate horseradish peroxidase-conjugated secondary antibodies (Santa Cruz Biotechnology, 1:3000 dilution). Blots were incubated with Western Lighting Chemiluminecense Reagent Plus (PerkinElmer Life Sciences) and chemiluminescence was detected using CL-X Posure Clear Blue X-ray Film (Thermo Scientific).

4.8. Griess (nitrite oxide) assay

Murine macrophage cells (RAW264.7) were plated in a 96-well plate in RPMI1640 and incubated at 37 °C for 24 h. The medium was changed, allowing cell induction by addition of compound and lipopolysaccharide (LPS) from *Escherichia coli* 055:B5 (LPS; Sigma-Aldrich) in the medium. After incubation, 50 μl of the supernatant was removed and incubated with the Griess reagent [150 μl; 0.5% sulfanilamide, 0.05% (*N*-1-naphthyl) ethylenediamine dihydrochloride, 2.5% H3PO4 and 97% H_2O by weight] for 30 min at room temperature in the dark. The absorbance is measured at 530 nm on a Dynex MRX II microplate spectrophotometer and calibrated using a standard curve constructed with sodium nitrite to yield NO_2^- concentration.

4.9. In vitro quantitative real-time PCR analysis

The bengamides A (**6**) and B (**7**) were evaluated in triplicate ($n = 3$) for their effects on nitrous oxide (NO) production ($n = 3$), TNFα ($n = 3$), IL-6 ($n = 3$) and MCP1 ($n = 3$). The results are presented as means ± standard deviation of the mean (STD). Differences in mean values between groups were analyzed by a one-way analysis of variance (ANOVA) using GraphPad Prism software (version 3.02 for Windows, GraphPad Software Inc., La Jolla, CA, USA). The statistical significance of mean differences was based on a p value of <0.05. A total RNA of 0.5 μg from RAW264.7 cells after treatment was exposed to DNase I treatment (Amersham Biosciences). cDNA was synthesised from DNase-treated RNA by reverse transcription. cDNAs from each experimental condition were pooled and PCR array analysis was performed according to the manufacturer protocol with the RT^2 Real-Time™ SYBR Green PCR Master Mix (SuperArray Bioscience Corporation). Quantitative real-time PCR array was performed on Mx3005P™ QPCR system (Stratagene, La Jolla, CA, USA). mRNA expression for each gene was normalized using the expression of GAPDH as a control housekeeping gene.

4.10. MTT cytotoxicity assay

Extract LC–MS–UV–ELSD library well fractions were tested at 20 μg/mL, respectively, based on assumed weights of 0.15 mg/well estimated from a 15 mg injection divided into two library plates (7.5 mg each) equally fractionated/50 wells ~0.15 mg/well. Pure compounds were tested using concentrations reported using a previously reported MTT assay[20] in murine macrophage (RAW264.7) cells to determine cytotoxic activity. Cells in 96-well plates in the required growth medium were treated with extracts dissolved in DMSO for 20 h (RAW264.7). After incubation, MTT solution was added to wells and incubated for another 2 h. Media were removed and DMSO was added to dissolve purple precipitates. Then plates were read at 570 nm using a plate reader.

Bengamide A (6): White powder; LRESITOFMS *m*/*z* 581.5 $[M-H_2O+H]^+$, 585.5 $[M+H]^+$. LC–MS and ^1H NMR data is provided in Figures. S13 and S14 (in the Supplementary data) and is equivalent to spectroscopic data reported previously.[38]
Bengamide B (7): White powder; LRESITOFMS *m*/*z* 621.5 $[M+Na]^+$. LC–MS and ^1H NMR data is provided in Figures. S15 and S16 and is equivalent to spectroscopic data reported previously.[38]
Bengamide E (8): Yellow oil; LRESITOFMS *m*/*z* 341.5 $[M-H_2O+H]^+$. LC–MS and ^1H NMR data is provided in Figures. S2 and S3 and is equivalent to spectroscopic data reported previously.[38]
Bengamide F (9): Clear oil; LRESITOFMS *m*/*z* 355.3 $[M-H_2O+H]^+$. LC–MS and ^1H NMR data is provided in Figures. S4 and S5 and is equivalent to spectroscopic data reported previously.[38]
LAF-389 (12): White powder; LRESITOFMS *m*/*z* 499.2 $[M+H]^+$. This compound was generously provided by Novartis Institute for Biomedical Research. LC–MS and ^1H NMR data is provided

in Figures. S17 and S18 and is equivalent to sprectroscopic data reported previously.[44]

Bengamide E′ (13): White powder; ^{1}H NMR data see Figures. S4–S10, and Table S1, Supplementary data; LRESITOFMS *m*/*z* 355.3 $[M-H_2O+H]^+$. HRESITOFMS $[M+H]^+ = C_{18}H_{33}N_2O_6$. Found, 373.2340, Calcd, 373.2331 (error = 0.0009 ppm).

Bengamide F′ (14): White powder; ^{1}H NMR data see Figures. S11 and S12, and Table S2, Supplementary data; LRESITOFMS *m*/*z* 369.3 $[M-H_2O+H]^+$. HRMS $[M+Na]^+$ = C19H34N2O6Na. Found, 409.22895, Calcd, 409.23091 (error = 4.78541 ppm).

Acknowledgements

This work was supported by Grants from the NIH R01 CA 47135 (PC), and NIH Fogarty International Center, International Cooperative Biodiversity Groups, Award number 1U01TW008160-01 and Agricultural Food Research Initiative of the National Institute of Food and Agriculture, USDA, Grant #35621-04750 (LFB) as well as MARC GM007910-31 (TLC). We are grateful to Katja M. Fisch for providing assistance in obtaining DSM strain 15898.

Supplementary data

An isolation scheme, two tables and nineteen figures are provided. This includes yields of the bengamides E, E′ and F′ from a 6 L grow up *M. virescens* culture and extraction, the LC–MS–UV–ELSD library of the active extract evaluated against the NF-κB luciferase and MTT cytotoxicity assays using murine macrophage (RAW 264.7) cells. Comparative LC–MS/ELSD traces and ^{1}H NMR spectra of the library fractions versus the bengamides E (**8**) and F (**9**) isolated from *J. coriacea* is included. Also provided is the 1D and 2D NMR data for bengamide E′ (**13**), ^{1}H and ^{13}C NMR data for bengamide F′ (**14**) followed by ^{1}H NMR and LC–MS data for the bengamides A (**6**), B (**7**) E (**8**), F (**9**) and LAF-389 (**12**).

Supplementary data associated with this article can be found, in the online version, at http://dx.doi.org/10.1016/j.bmc.2012.05.043.

References and notes

1. Newman, D. J.; Cragg, G. M. *J. Nat. Prod.* **2004**, *67*, 1216.
2. Weissman, K. J.; Muller, R. *Nat. Prod. Rep.* **2010**, *27*, 1276.
3. Huang, H.; Menefee, M.; Edgerly, M.; Zhuang, S.; Kotz, H.; Poruchynsky, M.; Huff, L. M.; Bates, S.; Fojo, T. *Clin. Cancer Res.* **2010**, *16*, 1634.
4. Waldmann, H.; Hu, T.-S.; Renner, S.; Menninger, S.; Tannert, R.; Oda, T. *Angew. Chem., Int. Ed.* **2008**, *47*, 6473.
5. Crews, P.; Manes, L. V.; Boehler, M. *Tetrahedron Lett.* **1986**, *27*, 2797.
6. Zabriskie, T. M.; Klocke, J. A.; Ireland, C. M.; Marcus, A. H.; Molinski, T. F.; Faulkner, D. J.; Xu, C.; Clardy, J. *J. Am. Chem. Soc.* **1986**, *108*, 3123.
7. Robinson, S. J.; Morinaka, B. I.; Amagata, T.; Tenney, K.; Bray, W. M.; Gassner, N. C.; Lokey, R. S.; Crews, P. *J. Med. Chem.* **2010**, *53*, 1651.
8. Holzinger, A.; Lutz-Meindl, U. *Cell Motil. Cytoskeleton* **2001**, *48*, 87.
9. Rachid, S.; Krug, D.; Kunze, B.; Kochems, I.; Scharfe, M.; Zabriskie, T. M.; Blocker, H.; Muller, R. *Chem. Biol.* **2006**, *13*, 667.
10. Sasse, F.; Kunze, B.; Gronewold, T. M. A.; Reichenbach, H. *J. Natl. Cancer Inst.* **1998**, *90*, 1559.
11. Kunze, B.; Jansen, R.; Sasse, F.; Hofle, G.; Reichenbach, H. *J. Antibiot.* **1995**, *48*, 1262.
12. Lebreton, S.; Jaunbergs, J.; Roth, M. G.; Ferguson, D. A.; De Brabander, J. K. *Bioorg. Med. Chem. Lett.* **2008**, *18*, 5879.
13. Erickson, K. L.; Beutler, J. A.; Cardellina, J. H.; Boyd, M. R. *J. Org. Chem.* **1997**, *62*, 8188.
14. Kunze, B.; Jansen, R.; Sasse, F.; Hofle, G.; Reichenbach, H. *J. Antibiot.* **1998**, *51*, 1075.
15. Li, Y.-Z.; Hu, W.; Zhang, Y.-Q.; Qiu, Z.-j.; Zhang, Y.; Wu, B.-H. *J. Microbiol. Methods* **2002**, *50*, 205.
16. Fudou, R.; Jojima, Y.; Iizuka, T.; Yamanaka, S. *J. Gen. Appl. Microbiol.* **2002**, *48*, 109.
17. Iizuka, T.; Jojima, Y.; Fudou, R.; Tokura, M.; Hiraishi, A.; Yamanaka, S. *Syst. Appl. Microbiol.* **2003**, *26*, 189.
18. Iizuka, T.; Jojima, Y.; Fudou, R.; Hiraishi, A.; Ahn, J.-W.; Yamanaka, S. *Int. J. Syst. Evol. Microbiol.* **2003**, *53*, 189.
19. Johnson, T. A.; Sohn, J.; Inman, W. D.; Estee, S. A.; Loveridge, S. T.; Vervoort, H. C.; Tenney, K.; Liu, J. K.; Ang, K. K. H.; Ratnam, J.; Bray, W. M.; Gassner, N. C.; Shen, Y. Y.; Lokey, R. S.; McKerrow, J. H.; Boundy-Mills, K.; Nukanto, A.; Kanti, A.; Julistiono, H.; Kardono, L. B. S.; Bjeldanes, L. F.; Crews, P. *J. Nat. Prod.* **2011**, *74*, 2545.
20. Wu, Q. X.; Crews, M. S.; Draskovic, M.; Sohn, J.; Johnson, T. A.; Tenney, K.; Valeriote, F. A.; Yao, X. J.; Bjeldanes, L. F.; Crews, P. *Org. Lett.* **2010**, *12*, 4458.
21. Ilyinskii, P. O.; Simon, M. A.; Czajak, S. C.; Lackner, A. A.; Desrosiers, R. C. *J. Virol.* **1997**, *71*, 1880.
22. Barger, S. W.; Horster, D.; Furukawa, K.; Goodman, Y.; Krieglstein, J.; Mattson, M. P. *Proc. Natl. Acad. Sci. U.S.A.* **1995**, *92*, 9328.
23. Gareus, R.; Kotsaki, E.; Xanthoulea, S.; van der Made, I.; Gijbels, M. J. J.; Kardakaris, R.; Polykratis, A.; Kollias, G.; de Winther, M. P. J.; Pasparakis, M. *Cell Metab.* **2008**, *8*, 372.
24. Tak, P. P.; Firestein, G. S. *J. Clin. Invest.* **2001**, *107*, 7.
25. Greten, F. R.; Karin, M. *Cancer Lett.* **2004**, *206*, 193.
26. Melisi, D.; Chiao, P. J. *Expert Opin. Ther. Targets* **2007**, *11*, 133.
27. Karin, M.; Yamamoto, Y.; Wang, Q. M. *Nat. Rev. Drug Disc.* **2004**, *3*, 17.
28. Gilmore, T. D. *Oncogene* **2006**, *25*, 6680.
29. Epinat, J. C.; Gilmore, T. D. *Oncogene* **1999**, *18*, 6896.
30. http://www.bu.edu/nf-kb/physiological-mediators/inhibitors/. Accessed 1/31/2012.
31. Gilmore, T. D.; Herscovitch, M. *Oncogene* **2006**, *25*, 6887.
32. Jin, H. Z.; Hwang, B. Y.; Kim, H. S.; Lee, J. H.; Kim, Y. H.; Lee, J. J. *J. Nat. Prod.* **2002**, *65*, 89.
33. Venkatesha, S. H.; Yu, H.; Rajaiah, R.; Tong, L.; Moudgil, K. D. *J. Biol. Chem.* **2011**, *286*, 15138.
34. Yang, H. J.; Chen, D.; Cui, Q. Z. C.; Yuan, X.; Dou, Q. P. *Cancer Res.* **2006**, *66*, 4758.
35. Hoffman, H.; Haag-Richter, S.; Kurz, M.; Tiertgen, H. *PCT Int. Appl.* 2005, WO 2005044803.
36. Thale, Z.; Kinder, F. R.; Bair, K. W.; Bontempo, J.; Czuchta, A. M.; Versace, R. W.; Phillips, P. E.; Sanders, M. L.; Wattanasin, S.; Crews, P. *J. Org. Chem.* **2001**, *66*, 1733.
37. Adamczeski, M.; Quinoa, E.; Crews, P. *J. Org. Chem.* **1990**, *55*, 240.
38. Adamczeski, M.; Quinoa, E.; Crews, P. *J. Am. Chem. Soc.* **1989**, *111*, 647.
39. Quinoa, E.; Adamczeski, M.; Crews, P.; Bakus, G. J. *J. Org. Chem.* **1986**, *51*, 4494.
40. Sarabia, F.; Martin-Galvez, F.; Chammaa, S.; Martin-Ortiz, L.; Sanchez-Ruiz, A. *J. Org. Chem.* **2010**, *75*, 5526.
41. Boeckman, R. K.; Clark, T. J.; Shook, B. C. *Org. Lett.* **2002**, *4*, 2109.
42. Mukai, C.; Moharram, S. M.; Kataoka, O.; Hanaoka, M. *J. Chem. Soc., Perkin Trans. 1* **1995**, 2849.
43. Liu, Q. J.; Li, H.; Chen, S. P.; Zhou, G. C. *Chin. Chem. Lett.* **2011**, *22*, 505.
44. Kinder, F. R.; Versace, R. W.; Bair, K. W.; Bontempo, J. M.; Cesarz, D.; Chen, S.; Crews, P.; Czuchta, A. M.; Jagoe, C. T.; Mou, Y.; Nemzek, R.; Phillips, P. E.; Tran, L. D.; Wang, R. M.; Weltchek, S. *J. Med. Chem.* **2001**, *44*, 3692.
45. Dumez, H.; Gall, H.; Capdeville, R.; Dutreix, C.; van Oosterom, A. T.; Giaccone, G. *Anticancer Drugs* **2007**, *18*, 219.
46. Towbin, H.; Bair, K. W.; DeCaprio, J. A.; Eck, M. J.; Kim, S.; Kinder, F. R.; Morollo, A.; Mueller, D. R.; Schindler, P.; Song, H. K.; van Oostrum, J.; Versace, R. W.; Voshol, H.; Wood, J.; Zabludoff, S.; Phillips, P. E. *J. Biol. Chem.* **2003**, *278*, 52964.
47. Hu, X.; Dang, Y.; Tenney, K.; Crews, P.; Tsai, C. W.; Sixt, K. M.; Cole, P. A.; Liu, J. O. *Chem. Biol.* **2007**, *14*, 764.
48. Lu, J. P.; Yuan, X. H.; Yuan, H.; Wang, W. L.; Wan, B. J.; Franzblau, S. G.; Ye, Q. Z. *ChemMedChem* **2011**, *6*, 1041.
49. Sakamoto, K. M.; Kim, K. B.; Kumagai, A.; Mercurio, F.; Crews, C. M.; Deshaies, R. J. *Proc. Natl. Acad. Sci. U. S. A.* **2001**, *98*, 8554.
50. Lu, H. T.; Ouyang, W. M.; Huang, C. S. *Mol. Cancer Res.* **2006**, *4*, 221.
51. Federico, A.; Morgillo, F.; Tuccillo, C.; Ciardiello, F.; Loguercio, C. *Int. J. Cancer* **2007**, *121*, 2381.
52. Kwok, B. H. B.; Koh, B.; Ndubuisi, M. I.; Elofsson, M.; Crews, C. M. *Chem. Biol.* **2001**, *8*, 759.
53. Bradley, J. R. *J. Pathol.* **2008**, *214*, 149.
54. Warren, M. A.; Shoemaker, S. F.; Shealy, D. J.; Bshar, W.; Ip, M. M. *Mol. Cancer Ther.* **2009**, *8*, 2655.
55. Gabay, C. *Arthritis Res. Ther.* **2006**, 8.
56. Schafer, Z. T.; Brugge, J. S. *J. Clin. Invest.* **2007**, *117*, 3660.
57. Viedt, C.; Dechend, R.; Fei, J.; Hansch, G. M.; Kreuzer, J.; Orth, S. R. *J. Am. Soc. Nephrol.* **2002**, *13*.
58. Kuroda, T.; Kitadai, Y.; Tanaka, S.; Yang, X. Q.; Mukaida, N.; Yoshihara, M.; Chayama, K. *Clin. Cancer Res.* **2005**, *11*, 7629.
59. Lu, J.; Yuan, X.; Ye, Q. *Eur. J. Med. Chem.* **2012**, *47*, 479.
60. Radisky, D. C.; Radisky, E. S.; Barrows, L. R.; Copp, B. R.; Kramer, R. A.; Ireland, C. M. *J. Am. Chem. Soc.* **1993**, *115*, 1632.
61. Ishibashi, M.; Iwasaki, T.; Imai, S.; Sakamoto, S.; Yamaguchi, K.; Ito, A. *J. Nat. Prod.* **2001**, *64*, 108.
62. Lane, A. L.; Moore, B. S. *Nat. Prod. Rep.* **2011**, *28*, 411.
63. Johnson, T. A.; Morgan, M. V. C.; Aratow, N. A.; Estee, S. A.; Sashidhara, K. V.; Loveridge, S. T.; Segraves, N. L.; Crews, P. *J. Nat. Prod.* **2010**, *73*, 359.
64. Johnson, T. A.; Tenney, K.; Cichewicz, R. H.; Morinaka, B. I.; White, K. N.; Amagata, T. A.; Subramanian, B.; Media, J.; Mooberry, S. L.; Valeriote, F. A.; Crews, P. *J. Med. Chem.* **2007**, *50*, 3795.